OPEN ACCESS

SHORT REPORT

A complex DICER1 syndrome phenotype associated with a germline pathogenic variant affecting the RNase IIIa domain of DICER1

Emeli Pontén ,[1] Sofia Frisk,[1,2] Fulya Taylan ,[1,2] Raquel Vaz,[1] Sandra Wessman,[3] Leanne de Kock ,[4] Niklas Pal,[5] William D Foulkes ,[4] Kristina Lagerstedt-Robinson ,[1,2] Ann Nordgren [1,2]

► Additional material is published online only. To view, please visit the journal online (http://dx.doi.org/10.1136/jmedgenet-2020-107385).

[1]Department of Molecular Medicine and Surgery (MMK), Karolinska Institute, Stockholm, Sweden
[2]Clinical Genetics, Karolinska University Hospital, Stockholm, Sweden
[3]Oncology-Pathology, Karolinska University Hospital, Stockholm, Sweden
[4]Departments of Human Genetics, Oncology, Medicine, McGill University, Montreal, Québec, Canada
[5]Department of Pediatric Oncology, Karolinska University Hospital, Stockholm, Sweden

Correspondence to
Professor Ann Nordgren, Dept of Molecular Medicine and Surgery (MMK), Karolinska Institute, 171 64 Stockholm, Sweden; ann.nordgren@ki.se

KL-R and AN are joint senior authors.

Received 5 August 2020
Revised 10 October 2020
Accepted 12 October 2020

To cite: Pontén E, Frisk S, Taylan F, *et al*. *J Med Genet* Epub ahead of print: [please include Day Month Year]. doi:10.1136/jmedgenet-2020-107385

ABSTRACT

Background Germline pathogenic variants in *DICER1* cause DICER1 syndrome, an autosomal dominant, pleiotropic tumour predisposition syndrome with variable expressivity and reduced penetrance for specific dysplastic and neoplastic lesions. Recently, a syndrome with the acronym GLOW (*G*lobal developmental delay, *L*ung cysts, *O*vergrowth, *W*ilms tumour) was described in two children with mosaic missense mutations in hotspot residues of the DICER1 RNase IIIb domain.

Methods Whole genome sequencing, exome sequencing, Sanger sequencing, digital PCR and a review of Wilms tumours with *DICER1* RNase III domain mutations were performed.

Results A de novo heterozygous c.4031C>T (p.S1344L) variant in the sequence encoding the RNase IIIa domain of *DICER1* was detected. Clinical investigations revealed a phenotype that resembles the GLOW subphenotype of DICER1 syndrome.

Conclusion The phenotypic overlap between patients with p.S1344L mutation and GLOW syndrome provide clinical support for recent discoveries that RNase IIIa-Ser1344 site mutations impede miRNA-5p biogenesis analogous to *DICER1* hotspot mutations in the RNase IIIb domain. We show that an individual with a heterozygous germline p.S1344L mutation has a severe form of DICER1 syndrome ('DICER1 syndrome plus'), with notable features of intellectual disability, macrocephaly, physical abnormalities, Wilms tumour and a well-differentiated fetal adenocarcinoma of the lung.

INTRODUCTION

The *DICER1* (MIM *606241) gene located at 14q32.13 is important for embryogenesis and early somatic development. Residing in the cytoplasm, the DICER1 protein is an endoribonuclease (RNase) III cleaving double-stranded RNA. The enzyme is crucial for producing miRNAs, as it processes precursor strands (pre-miRNA) whereby two single-stranded miRNA molecules are produced, named by their prime end origin (3p/5p miRNA).[1]

DICER1 syndrome (MIM #601200) is an autosomal dominant, pleiotropic tumour predisposition syndrome with variable expression and reduced penetrance of benign and malignant tumours, commonly pleuropulmonary blastoma (PPB), cystic nephroma, Sertoli-Leydig cell tumour and hyperplastic proliferations such as multinodular goitre. The most frequently observed mechanism underlying tumour formation in DICER1 syndrome is the presence of biallelic alterations that include germline loss of function (LOF) pathogenic variants, combined with somatic in trans mutations in the sequence encoding the hotspot residues of the RNase IIIb domain.[1 2]

Missense mutations occurring in exons encoding the DICER1 RNase IIIb domain, either involving or adjacent to catalytically active metal-ion binding residues including p.E1705, p.D1709, p.G1809, p.D1810, p.E1813 and p.D1713 are recognised as cancer hotspot loci. Alterations of these RNase IIIb residues cause neomorphic alleles, reported to be functionally equivalent with respect to miRNA biogenesis.[2] These alterations interfere with the canonical processing of miRNA precursors, resulting in a relative excess of 3p-miRNA and a depletion of 5p-miRNA.[3] It has recently been revealed through evolutionary and structural coupling analyses that RNase IIIa-S1344 site is in close proximity to the active cleft of RNase IIIb domain and that a mutation in RNase IIIa-S1344 exhibit the same pattern of 5p-miRNA loss as that resulting from RNase IIIb hotspot mutations.[4] In 2014, Klein *et al* proposed a new *DICER1* related syndrome with the acronym GLOW (Global developmental delay, Lung cysts, Overgrowth, Wilms tumour), describing two children with mosaic missense hotspot mutations in *DICER1* affecting the RNase IIIb domain. A highly penetrant and severe phenotype has been shown in patients with mosaic[5 6] or germline[7] RNase IIIb mutations, compared with patients with classic DICER1 syndrome caused by germline LOF pathogenic variants.

Here, we show evidence that the germline c.4031C>T (p.S1344L) mutation in *DICER1* causes a severe subtype of DICER1 syndrome with intellectual disability (ID), macrocephaly, extensive bilateral lung cysts, early onset of Wilms tumour and well-differentiated fetal lung adenocarcinoma—a clinical spectrum similar to, but distinct from, the phenotype reported in two patients with GLOW syndrome with postzygotic hotspot mutations in exons encoding the RNase IIIb domain.

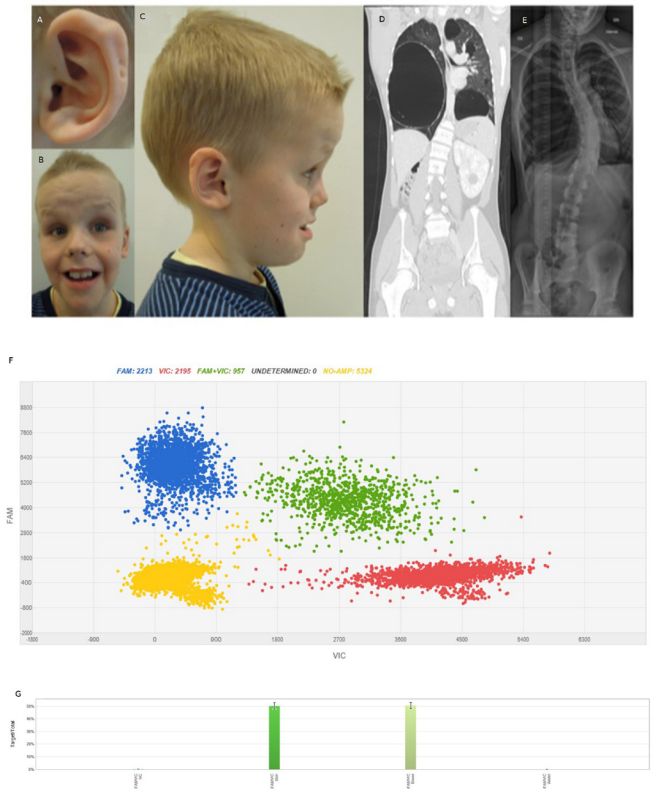

Figure 1 Patient characteristics. Photographs of the patient at 10.5 years of age showing (A) posterior ear pits of left helix, (B) a high, broad, furrowed forehead, mild hypertelorism, short, upturned nose, facial nevi, large mouth and teeth, (C) profile portrait of the patient showing macrocephaly and posterior ear pits of the right helix. (D) CT scan of the patient at 16 years of age showing bilateral large cysts and a cystic nephroma in the remaining enlarged kidney. (E) Chest X-ray of the patient at 16 years of age showing left convex thoracic scoliosis. (F) dPCR results of DNA from skin biopsy from the patient. Blue cluster represents amplification of the target region—the mutant allele c.4031C>T. Red signals represent the internal reference control and green signals both mutant and reference alleles. Yellow cluster represents the wells where no amplification signal was detected. (G) Mutant frequency comparison. X-axis and Y-axis show the intensities of signals VIC and FAM channels. Columns display the distribution of 50% of the c.4031C>T variant in DNA from skin and blood from the patient. Left column—skin, right column—peripheral blood.

MATERIALS AND METHODS

Methods

Genomic DNA was extracted from peripheral blood, skin, saliva, oral mucosa, fresh tumour tissue and formalin-fixed, paraffin-embedded tumour tissue using standard protocols. DNA from both parents was extracted from peripheral blood.

Sequencing and bioinformatic analysis

Standard 30x whole genome sequencing (WGS), exome sequencing (ES) and bioinformatic analysis were performed at Clinical Genomics, SciLifeLab, Stockholm, using the Illumina HiSeq X Ten platform. Single nucleotide variants were called using Mutation Identification Pipeline. Variants were filtered, removing variants with a frequency over 1% in the general population.[8] A constructed gene panel based on HPO-terms (Macrocephaly HP:0000256, Polydactyly HP:0010442, Nephroblastoma HP:0002667) consisting of in total 476 genes were analysed regarding variants affecting coding regions or splicing (online supplemental table 1). The clinically relevant sequence variant was verified in the patient using Sanger sequencing. Carrier testing of the parents was performed using Sanger sequencing.

Digital PCR

Genomic DNA extracted from blood, skin, saliva and oral mucosa were amplified using 1X QuantStudio 3D Digital PCR Master mix and commercially available TaqMan assay for *DICER1* c.4031C>T mutation (Applied Biosystems, California, USA). DNA was quantified using Qubit fluorometry (Thermo Fisher Scientific, Massachusetts, USA). Then 14.6 μL of PCR reaction mixes were loaded into QS3D Digital 20K V2 chips (Applied Biosystems). Protocol was followed as previously described.[9] Digital PCR data were analysed using PoissonPlus algorithm (V.4.4.10) with a 95% CI and a desired precision of 10% by QuantStudio 3D AnalysisSuite (V.3.1.2-PRC-build-03).

RESULTS

Clinical description

The patient is the first child from healthy, non-consanguineous parents with unremarkable family history. He was born at gestational week 39 after a difficult delivery due to macrocephaly (Apgar 1-3-7). The birth weight was 3752 g, length 53 cm and head circumference 42 cm (>99th percentile). Clinical findings at birth included two blood vessels in the umbilical cord, undescended testis, inguinal hernia, postaxial polydactyly, ear pits and rocker bottom feet. Fontanel closure was late and he had difficulties breast feeding. At 15 months of age, he was diagnosed with a right-sided Wilms tumour (classic triphasic nephroblastoma with all three classic histological elements). Abdominal ultrasound also revealed a cyst of benign appearance in his left kidney. A lung scan showed multiple large cysts and a suspected Wilms tumour metastasis. A lobectomy of the middle lobe was performed to remove the tumour and three cysts. Owing to suspicion of additional metastasis, another thoracotomy was performed and two cysts in the right lower lobe were removed. The five removed lung cysts were diagnosed as benign fibrotic emphysematous alterations with bullous, cystic character. The pathologic-anatomic diagnosis of the lesion in the middle lobe was initially Wilms tumour metastasis, but following the identification of the pathogenic germline *DICER1* variant, pathology review determined that the correct diagnosis was well-differentiated fetal adenocarcinoma. Re-examination of radiographic findings, also after the DICER1 syndrome diagnosis, revealed a suspicion of a multiloculated cystic nephroma in the remaining kidney. The patient received postoperative chemotherapy and has been tumor-free since 2006. He had a late psychomotor development, started to walk at 3 years of age and spoke full sentences at 5 years. MRI of the brain was performed at 12 years of age and revealed signs of white matter reduction including a thin corpus callosum. At 18 years of age, he has normal length and weight, and a pronounced macrocephaly (>99th percentile). Dysmorphic features include a broad and furrowed forehead, wide mouth, tooth anomalies, doughy, soft skin and multiple nevi. Furthermore, he has ID, autism, behavioural problems and has required surgical treatment due to a left-convex thoracic scoliosis (figure 1, table 1).

Genetic findings

WGS analysis after bioinformatic filtering revealed four sequence variants for clinical review (online supplemental table 2). The

Table 1 All known patients with germline or mosaic RNase III domain hotspot mutations

DICER1 syndrome+phenotype	Klein *et al*[5] Pat 1	Klein *et al*. Pat 2[5]	Pontén *et al (the present study)*r	Carlens *et al*[10]	de Kock *et al*.[6] Pat 1 (Brenneman *et al*[11] Pat 102)	de Kock *et al*[6] Pat 2 (Brenneman *et al*[11] Pat 105)	de *Kock et al*[6] Pat 3	de Kock *et al*[6] Pat 4 Brenneman *et al*[11] Pat 120)	de Kock *et al*[7] Pat 12	Brenneman *et al* [11] Pat 101	Brenneman *et al* [11] Pat 103	Brenneman *et al*.[11] Pat 104	Brenneman *et al*[11] Pat 123
Patient age and sex (,if reported)	5 y M	14 m M	18 y M	6 y F	10.9 y M	17.2 y F	6.8 y F	4.1 y M	21 m M	9 y	14 y	13 y F	8 y
DICER1 RNase III hotspot mutation: domain/germline or mosaic	c.5138A>T p.D1713V RNase IIIb domain mosaic	c.5125G>T p.D1709Y RNase IIIb domain mosaic	c.4031C>T p.S1344L RNase IIIa domain germline	c.4031C>T p.S1344L RNase IIIa domain germline	c.5125G>A p.D1709N RNase IIIb domain mosaic	c.5437G>C p.E1813Q RNase IIIb domain mosaic	c.5439G>C p.E1813D RNase IIIb domain mosaic	c.5425G>Ap.G1809R RNase IIIb domain mosaic	c.5125G>C p.D1709H RNase IIIb domain germline	c.5126A>G; p.D1709G RNase IIIb domain mosaic	c.5125G>A; p.D1709N RNase IIIb domain mosaic	c.5428G>T; p.D1810Y RNase IIIb domain mosaic	c.5113G>A; p.E1705K RNase IIIb domain mosaic
DICER1 RNase III hotspot mutation: tissue distribution and VAF	Blood: (21%) Normal kidney: (35%) Wilms tumour:(37%)	Blood: (28%) Normal kidney:(35%) Wilms tumour:(47%)	Blood: (50%) Skin: (50%) Buccal cells: (50%) Saliva: (50%) Kidney tumour: (87%) Lung tumour: (90%)	Blood: (heterozygous)	Blood: (4.6%) Skin: (4.23%–7.13%) Saliva: (2.78%) Normal brain: (11.52%) Lymph node: (0%) NCMH: (17.72%) Type I PPB: (34.24%) Type II PPB: (43.84%) Brain PPB metastasis: (14.97%–51%)	Blood: (0.04%) Urine: (0.4%–0.66%) Saliva: (0.25%–0.27%) Hair: (0.24%) Lung cysts: (0%) Follicular thyroid ca:(66.6%–74.53%) SLCT (right): (76.8%–87.33%) SLCT (left): (31.8%–44.48%) NCMH: (29.3%–30.55%)	Blood: (0–0.04%) Normal right kidney #1: (3.26%–4.75%) Normal right kidney #2: (12.86%–14.55%) CN left kidney: (7.62%) Maldevelopmental lesion right kidney: (56.24%) Juvenile polyps: (38.9%) NCMH: (27.73%)	Blood: (0%–0.2%) Hair: (0.02%) Saliva: (0%–0.04%) Reactive lung (left): (0.35%–1%) Reactive lung (right): (6.93%–7.08%) Type II PPB: (37%–37.84%)	Blood: (heterozygous) Pituitary blastoma: (NR)	Blood: (NR) Normal lymph node: (15.2%)	Blood: (0.28%) CN: (14.9%) Type Ir PPB: (16.2%) Small intestine, polyps: (17.5%)	Blood: (0.21%) Normal Fallopian tube: (7.19%) Type Ir PPB: (27.8%) CN: (29.2%) SLCT (right): (34.2%) SLCT (left): (92.4%)	Blood: (ND) Normal ureter: (13%) Type I PPB:(24%) CN: (35%)
DICER1 LOF mutation: tissue distribution/(allele frequency)	Blood: (ND) Normal kidney: (ND) Wilms tumour: c.1304C>A, p.P453H and c.5692A>G p.R1898G (variable)	Blood: (ND) Normal kidney: (ND) Wilms tumour: (ND)	Blood: (ND) Kidney tumour: 0.61 Mb deletion (approx. 50%)	Blood: (ND)	Blood: (ND) PPB metastasis in brain: (allele loss)	Blood: (ND) NCMH: (ND) Thyroid ca: (allele loss) SLCT (right): (allele loss) SLCT (left): c.4626-4626delG; p.Q1542Hfs*18: (21.7%–44.48%) NCMH: c.4458_4458delA p.K1486Nfs*4 (NR)	NCMH: c.4651-4652insTGCT; p.E1551Vfs*7 (NR)	Blood: (ND) Reactive lung: (ND) Type II PPB: c.1966C>T; p.R656* (NR)	Blood: (ND) Pituitary blastoma: (allele loss)	Blood: (ND) Normal Lymph node: (ND)	Blood: (ND) CN: c.1129G>A; p.V377I(3.1%) Type Ir PPB: c.1200G>A; p.W400* (4.1%) Small intestine polyp: c.96G>A; p.W32* (3%)	Blood: (ND) Normal Fallopian tube: (ND) Type Ir PPB: (ND) CN: c.1711delT; p.S571Vfs*16 (21.8%) SLCT (right): c.1775delA; p.K592Mfs*15 (36.2%) SLCT (left): (allele loss)	Blood: (ND) Normal ureter: (ND) Type I PPB: (allele loss) CN: (allele loss)
Intellectual impairment	DD	DD	ID	ID	ND	ND	ND	ND	ND	NR	NR	NR	NR
Autism	Yes	NR	Yes	Yes	NR	NR	NR	NR	NR	NR	NR	NR	NR
Hypotonia	Yes	Yes	Yes	Yes	NR	NR	NR	NR	NR	NR	NR	NR	NR
Overgrowth	Macrocephaly/Global	Macrocephaly/Global	Macrocephaly	Macrocephaly	ND	ND	ND	ND	ND	NR	NR	NR	NR
Birth weight	4904 g (>99th percentile)	2920g (18th percentile)	3752 g (79th percentile)	4430g (>99th percentile)	NR	NR	NR	NR	NR	NR	NR	NR	NR
Birth length	NR	NR	53 cm (95th percentile)	56 cm (>99th percentile)	NR	NR	NR	NR	NR	NR	NR	NR	NR
OFC at birth	NR	NR	42 cm (>99th percentile)	42 cm (>99th percentile)	NR	NR	NR	NR	NR	NR	NR	NR	NR
Growth parameters: weight (w)/length (L)/head size (OFC)	28m: W 15.5kg (91.9th percentile) L 95 cm (95.5th percentile) OFC 55 cm (>99th percentile)	14m: W 13.5 kg (>99th percentile) L 81 cm (95.6th percentile) OFC 53 cm (>99th percentile)	18 y: W normal L normal OFC 62 cm (>99th percentile)	6 y: W 15.8 kg (3.6th percentile) L 112 cm (27.4th percentile)	NR	NR	NR	NR	NR	NR	NR	NR	NR
Nephromegaly	Yes	Yes	NR	No	NR	NR	NR	NR	NR	NR	NR	NR	NR
Renal cysts	Multiple small cysts	Multiloculated cystic mass (left)	CN at 8 y	NR	NR	Hamartomatous bilat renal cysts at 1 y 1 m	CN at 1 y	NR	Yes	CN at 1 y 3 m	CN at 1 y	CN at 1 y	CN at 1 y 6 m
Lung cysts/PPB	Lung cysts/PPB	Lung cysts/PPB	Type I PPB	Lung cysts at 11 m	Type I PPB Type II PPB	Benign multifocal bilat lung cysts at 1 y 1 m	Type I PPB (right) Lung cysts (left)	Lung cysts (right) Type I PPB (left) at 11 m, Type II PPB at 4 y	Type II PPB	PPB at 1 y 3 m	Type Ir PPB at 11 m	Type Ir PPB at 5 m	Type I PPB at 1 y 8 m
Hypertelorism	Yes	(Yes)	(Yes)	Yes	NR	NR	NR	NR	NR	NR	NR	NR	NR
Prominent forehead	Yes	Yes	Yes	Yes	NR	NR	NR	NR	NR	NR	NR	NR	NR
Anteverted nares	Yes	NR	Yes	NR	NR	NR	NR	NR	NR	NR	NR	NR	NR
Flat nasal bridge	Yes	Yes	Yes	NR	NR	NR	NR	NR	NR	NR	NR	NR	NR
Micrognathia	(Yes)	NR	(Yes)	NR	NR	NR	NR	NR	NR	NR	NR	NR	NR
Macrosomia	NR	NR	Yes	Yes	NR	NR	NR	NR	NR	NR	NR	NR	NR
Pits	Sacral dimple+dimples on sides of ankles	Ear pit (left)	Ear pits, posterior helix (left)	NR	NR	NR	NR	NR	NR	NR	NR	NR	NR
Skin findings	Doughy hands Fat pads on feet Pronounced plantar creases	NR	Soft skin Doughy soft hands Furrowed forehead Multiple nevi	NR	NR	NR	NR	NR	NR	NR	NR	NR	NR
Skeletal abnormalities	Pectus excavatum Kyphosis	NR	Scoliosis Polydactyly	Narrow thorax Increased intermammillary distance Prominent sternum	NR	NR	NR	NR	NR	NR	NR	NR	NR
Increased CSF space	Yes	Yes	Yes	Yes	NR	NR	NR	NR	NR	NR	NR	NR	NR
Fontanel	Large anterior fontanel	NR	Late fontanel closure	NR	NR	NR	NR	NR	NR	NR	NR	NR	NR
Hernia	Inguinal and umbilical	Inguinal	Inguinal	NR	NR	NR	NR	NR	NR	NR	NR	NR	NR
Brain imaging	Enlarged lateral and third ventricles	Mild volume loss	Mild volume loss Thin corpus callosum Cyst	Enlarged lateral ventricles Hydrocephalus	NR	NR	NR	NR	NR	NR	NR	NR	NR
Wilms tumour (age of Dx)	Bilateral 9m/5 y	Bilateral 1 y 1 m/2 y 6 m	Bilateral 1 y 3 m/1 y6 m	Unilateral 11 m	ND	ND	ND	ND	ND	ND	ND	ND	ND

Continued

Table 1 Continued

DICER1 syndrome+phenotype	Klein *et al*[5] Pat 1	Klein *et al*. Pat 2[5]	Pontén *et al (the present study)*/r	Carlens *et al*[10]	de Kock *et al*.[6] Pat 1 (Brenneman *et al*[11] Pat 102)	de Kock *et al*.[6] Pat 2 (Brenneman *et al*,[11] Pat 105)	de Kock *et al*[8] Pat 3	de Kock *et al*.[6] Pat 4 Brenneman *et al*[11] Pat 120)	de Kock *et al*[7] Pat 12	Brenneman *et al*.[11] Pat 101	Brenneman *et al*.[11] Pat 103	Brenneman *et al*.[11] Pat 104	Brenneman *et al*.[11] Pat 123
Small intestine, polyps	NR	NR	NR	NR	Yes	NR	Hamartomatous juvenile intestinal polyps at 6 m	NR	NR	Yes	Yes	Yes	NR
Additional cysts or tumours	NR	NR	NR		NCMH at 8 y Testicular cyst at birth PPB brain metastasis	NCMH at 15 y Pineoblastoma at 7 y Follicular papillary thyroid carcinoma at 10 y Bilat SLCT at 13 y and 15 y Ciliary body medulloepithelioma at 17 y	NCMH at 6 y	NR		Pituitary blastoma at 8 m	Hodgkin lymphoma at 7 y	Pelvic sarcoma at 14 y	SLCT bilat at 5 y and 13 y Thyroid nodules at 7 y	NR
Other clinical findings	Respiratory distress	Pre-eclampsia in mother	Reduced fetal movement during pregnancy Retentio testis Rocker bottom feet Language impairment Large teeth Two blood vessels in umbilical cord Pulmonary embolism after scoliosis surgery	Low set ears Pulmonary infections Myopathic facies with ptosis and open mouth	Scrotal web at birth Enteritis cystica profunda at 9 m	Left ocular pre-phtisisical changes, vascular mass Recurrent retinal detachment	Renal medullary malformation with disorganised collecting system and dilated lymphatic vessels	NR	NR	NR	NR	NR	NR

CN, cystic nephroma; DD, developmental delay; ID, intellectual disability; LOF, loss of function; m, month; NCMH, nasal chondromesenchymal hamartoma; ND, none detected; NR, not reported; OFC, occipital frontal circumference; PPB, pleuropulmonary blastoma; SLCT, Sertoli-Leydig cell tumour; VAF, variant allele frequency; y, year.

only clinically relevant variant was a heterozygous sequence variant in exon 21 of *DICER1;* NM_030621.4: c.4031C>T, (p.S1344L). The variant was verified and segregation analysis was performed using Sanger sequencing. Neither of the parents were carriers of this variant (data not shown). Digital PCR was performed on patient-DNA from buccal cells (not shown), saliva (not shown), blood and skin (figure 1), which showed a mutant allelic frequency of 50% in all samples, thus excluding mosaicism of the mutation. ES of DNA prepared from kidney and lung tumour tissue revealed that the germline heterozygous mutation c.4031C>T in *DICER1* was more abundant in the tumour tissue, 87% and 90%, respectively. In order to verify loss of heterozygosity (LOH) in the tumour, DNA from the fresh tissue (kidney tumour) was subjected to WGS. WGS data confirmed a 0.61 Mb deletion covering the whole *DICER1* gene (Chr14(Hg19): g.95247243_95858197del).

ES of the well-differentiated fetal lung adenocarcinoma revealed distinct tumour-only single nucleotide variants that distinguished it from the Wilms tumour and confirmed its separate nature.

DISCUSSION

We show that a heterozygous germline mutation c.4031C>T (p.S1344L) in the RNase IIIa domain of DICER1 is compatible with life, and causes a complex 'DICER1 syndrome plus' phenotype with extensive bilateral and multilobar lung cysts, PPB, cystic nephroma, Wilms tumour, well-differentiated fetal lung adenocarcinoma, ID, macrocephaly, ear pits and other physical anomalies. This phenotype closely resembles reported clinical findings of a patient with the identical germline p.S1344L pathogenic variant presented at a paediatric pneumology association meeting in Vienna.[10] There are also close similarities to the phenotype described in two children with GLOW syndrome and mosaic hotspot mutations in the RNase IIIb domain,[5] although the postnatal overgrowth was more pronounced in the individuals with GLOW syndrome. Thus, the phenotype of the widely expressed germline RNase IIIa-S1344L variant resembles the extreme end of the phenotypes associated with mosaic hotspot mutations in the sequence encoding the RNase IIIb domain of DICER1.[11] This strongly supports previous somatic findings from integrated genetic analysis and in vitro cell experiments in cancer cells, where the RNase IIIa-S1344L mutation functionally perturbs RNase IIIb catalytic activity.[2 4] The observation that only a minority of reported germline (n=1) or mosaic (n=10) RNase IIIb mutations are associated with the so-called GLOW phenotype (table 1), suggests that these mutations result in severe but highly pleiotropic phenotypes that cannot be predicted from the genotype.[2 5 6 11] It will be important to determine whether, in contrast, RNase IIIa hotspot mutations invariably result in a severe 'DICER1 syndrome plus' phenotype.

In support of a potentially distinct functional consequence of RNase IIIa hotspot mutations, compared with RNase IIIb mutations, RNase IIIa catalytic site mutations are rare in cancers and RNase IIIa-S1344L is the only recurring cancer hotspot mutation that occurs in this domain. To date, p.S1344L mutations have been described in 15 tumours. Interestingly, the types of tumours which develop due to *DICER1* hotspot mutations are unevenly distributed among the targeted tissues. In the 15 tumours with p.S1344L in the RNase IIIa domain, there were 4 Wilms tumours, 4 malignant melanomas, 1 Merkel cell carcinoma, 3 endometroid carcinomas, 2 colorectal cancers and 1 cholangiocarcinoma.[10 12–15] Tumours bearing RNase IIIa-S1344L hotspot mutations are most commonly malignant melanomas

(4/15; 27%) in contrast to tumours bearing hotspot mutations in the RNase IIIb domain (2/318; 0.6%).[4 15] This indicates that hotspot mutations in different RNase III domains of DICER1 cause tissue-specific susceptibilities to develop certain tumours.

This is the second well-differentiated fetal lung adenocarcinoma reported in DICER1 syndrome.[16–18] Here, the diagnosis was made on the basis of glycogen-rich neoplastic glands and tubules resembling fetal lung tissue (at 10–15 weeks gestation). In contrast to biphasic PPB, the adjacent stroma is benign.

In addition to our patient, we identified 27 sequenced Wilms tumours with RNase IIIa or RNase IIIb domain hotspot mutations; in 17 of 28 (61%) there was no alteration on the other allele, while 11 of 28 (39%) had two mutations. One tumour with a germline RNase IIIa hotspot mutation did not undergo somatic testing (online supplemental table 3). Further studies are needed to determine if the sequenced Wilms tumours that lacked somatic alterations on the other allele could have copy neutral LOH or a deletion as described in our patient, or other genetic aberrations that escaped detection by the methods used.

Non-tumour-related phenotypes occur in DICER1 syndrome; macrocephaly has recently been described in 28/67 (42%) of patients with the syndrome in a single study.[19] General overgrowth is more pronounced in patients with GLOW syndrome,[5] while patients with RNase IIIa-S1344L mutations only present with macrocephaly.[10] Recently, Klein *et al* reported activation of the phosphatidylinositol 3-kinase (PI3K)/AKT/mammalian target of rapamycin (mTOR) pathway in genetically modified cells with hotspot mutations in the RNase IIIb domain associated with GLOW syndrome.[20] It is noteworthy that some patients with mutations in the PI3K/AKT/mTOR pathway have overlapping symptoms with our patient, such as polydactyly in patients with mutations in *AKT3* or *PIK3CA*, and multiple nevi, macrocephaly and ID seen in *PTEN* and *PIK3CA*-related disorders. Posterior helical pits are rare and have previously been described in Beckwith-Wiedemann syndrome, Simpson-Golabi-Behmel syndrome and GLOW syndrome, all of which are cancer predisposition syndromes with a risk of developing Wilms tumour. In patients with Beckwith-Wiedemann syndrome and *CDKN1C* mutations, an extended phenotype including ear pits and polydactyly has been described. To date, ID/developmental delay has been reported in at least nine patients with large deletions encompassing several genes including *DICER1*,[21–27] and in three patients with RNase IIIb or RNase IIIa-S1344L hotspot mutations.[5 10]

The highly penetrant and severe phenotypes described in patients with germline or mosaic RNase III domain mutations[5 6] may be explained by the likelihood of a second somatic mutation stochastically occurring in any part of *DICER1* being greater than the reverse succession normally seen in DICER1 syndrome, in combination with tissue-specific neomorphic effects of the specific heterozygous RNase III domain mutations.[11]

In conclusion, germline RNase IIIa-S1344L pathogenic variants result in a "DICER1 syndrome plus" phenotype that in addition to classic features, also includes ID and ear pits. The conferred phenotype is similar, but not identical to that of early post zygotic DICER1 RNase IIIb hotspot mutations.

Acknowledgements The authors would like to thank the family of the described patient for their participation. Additional results published here are in part based on data generated by the TCGA Research Network: https://www.cancer.gov/tcga.

Contributors AN coordinated the study. AN and KLR performed WGS analyses. NP provided clinical care. SW, SF, WDF, AN and NP performed clinical and pathological phenotyping. SF and FT performed digital PCR. EP, SF, FT, AN, RV, NP, WDF, LdK and KLR contributed with data collection, interpretation and discussion of results. EP and AN wrote the manuscript in consultation with all authors.

Funding This work was supported by grants from the Swedish Childhood Cancer Fund, the Swedish Cancer Society, the Cancer Society of Stockholm, the Swedish Research Council, Berth von Kantzow's Foundation and The Hållsten Research Foundation.

Competing interests WDF reports support from AstraZeneca, outside the submitted work (VUS classification project in breast cancer gene sequencing project).

Patient consent for publication Parental/guardian consent obtained.

Ethics approval The local Ethics Committee at Karolinska Institute approved the study (Dnr 2012-2106-31/4), which followed the tenets of the Declaration of Helsinki. Written informed consent was obtained from the parents.

Provenance and peer review Not commissioned; externally peer reviewed.

ORCID iDs
Emeli Pontén http://orcid.org/0000-0002-9174-9804
Fulya Taylan http://orcid.org/0000-0002-2907-0235
Leanne de Kock http://orcid.org/0000-0001-7314-1371
William D Foulkes http://orcid.org/0000-0001-7427-4651
Kristina Lagerstedt-Robinson http://orcid.org/0000-0001-9848-0468
Ann Nordgren http://orcid.org/0000-0003-3285-4281

REFERENCES

1 Foulkes WD, Priest JR, Duchaine TF. DICER1: mutations, microRNAs and mechanisms. *Nat Rev Cancer* 2014;14:662–72.
2 de Kock L, Wu MK, Foulkes WD. Ten years of DICER1 mutations: Provenance, distribution, and associated phenotypes. *Hum Mutat* 2019;40:1939–53.
3 Rakheja D, Chen KS, Liu Y, Shukla AA, Schmid V, Chang T-C, Khokhar S, Wickiser JE, Karandikar NJ, Malter JS, Mendell JT, Amatruda JF. Somatic mutations in Drosha and DICER1 impair microRNA biogenesis through distinct mechanisms in Wilms tumours. *Nat Commun* 2014;2:4802.
4 Vedanayagam J, Chatila WK, Aksoy BA, Majumdar S, Skanderup AJ, Demir E, Schultz N, Sander C, Lai EC. Cancer-Associated mutations in DICER1 RNase IIIA and IIIB domains exert similar effects on miRNA biogenesis. *Nat Commun* 2019;10:3682.
5 Klein S, Lee H, Ghahremani S, Kempert P, Ischander M, Teitell MA, Nelson SF, Martinez-Agosto JA. Expanding the phenotype of mutations in DICER1: mosaic missense mutations in the RNase IIIB domain of DICER1 cause glow syndrome. *J Med Genet* 2014;51:294–302.
6 de Kock L, Wang YC, Revil T, Badescu D, Rivera B, Sabbaghian N, Wu M, Weber E, Sandoval C, Hopman SMJ, Merks JHM, van Hagen JM, Bouts AHM, Plager DA, Ramasubramanian A, Forsmark L, Doyle KL, Toler T, Callahan J, Engelenberg C, Bouron-Dal Soglio D, Priest JR, Ragoussis J, Foulkes WD. High-sensitivity sequencing reveals multi-organ somatic mosaicism causing DICER1 syndrome. *J Med Genet* 2016;53:43–52.
7 de Kock L, Sabbaghian N, Plourde F, Srivastava A, Weber E, Bouron-Dal Soglio D, Hamel N, Choi JH, Park S-H, Deal CL, Kelsey MM, Dishop MK, Esbenshade A, Kuttesch JF, Jacques TS, Perry A, Leichter H, Maeder P, Brundler M-A, Warner J, Neal J, Zacharin M, Korbonits M, Cole T, Traunecker H, McLean TW, Rotondo F, Lepage P, Albrecht S, Horvath E, Kovacs K, Priest JR, Foulkes WD. Pituitary blastoma: a pathognomonic feature of germ-line DICER1 mutations. *Acta Neuropathol* 2014;128:111–22.
8 Karczewski KJ, Francioli LC, Tiao G, Cummings BB, Alföldi J, Wang Q, Collins RL, Laricchia KM, Ganna A, Birnbaum DP, Gauthier LD, Brand H, Solomonson M, Watts NA, Rhodes D, Singer-Berk M, England EM, Seaby EG, Kosmicki JA, Walters RK, Tashman K, Farjoun Y, Banks E, Poterba T, Wang A, Seed C, Whiffin N, Chong JX, Samocha KE, Pierce-Hoffman E, Zappala Z, O'Donnell-Luria AH, Minikel EV, Weisburd B, Lek M, Ware JS, Vittal C, Armean IM, Bergelson L, Cibulskis K, Connolly KM, Covarrubias M, Donnelly S, Ferriera S, Gabriel S, Gentry J, Gupta N, Jeandet T, Kaplan D, Llanwarne C, Munshi R, Novod S, Petrillo N, Roazen D, Ruano-Rubio V, Saltzman A, Schleicher M, Soto J, Tibbetts K, Tolonen C, Wade G, Talkowski ME, Neale BM, Daly MJ, MacArthur DG, Genome Aggregation Database Consortium. The mutational constraint spectrum quantified from variation in 141,456 humans. *Nature* 2020;581:434–43.

9 Frisk S, Taylan F, Blaszczyk I, Nennesmo I, Annerén G, Herm B, Stattin E-L, Zachariadis V, Lindstrand A, Tesi B, Laurell T, Nordgren A. Early activating somatic PIK3CA mutations promote ectopic muscle development and upper limb overgrowth. *Clin Genet* 2019;96:118–25.
10 Carlens J KC, Ahrens F, Griese M, Schwerk N. *Zeitschrift der gesellschaft für pädiatrische pneumologie*, 2018: 36–41.
11 Brenneman M, Field A, Yang J, Williams G, Doros L, Rossi C, Schultz KA, Rosenberg A, Ivanovich J, Turner J, Gordish-Dressman H, Stewart D, Yu W, Harris A, Schoettler P, Goodfellow P, Dehner L, Messinger Y, Hill DA. Temporal order of RNase IIIb and loss-of-function mutations during development determines phenotype in pleuropulmonary blastoma / *DICER1* syndrome: a unique variant of the two-hit tumor suppression model. *F1000Res* 2015;4.
12 Gadd S, Huff V, Walz AL, Ooms AHAG, Armstrong AE, Gerhard DS, Smith MA, Auvil JMG, Meerzaman D, Chen Q-R, Hsu CH, Yan C, Nguyen C, Hu Y, Hermida LC, Davidsen T, Gesuwan P, Ma Y, Zong Z, Mungall AJ, Moore RA, Marra MA, Dome JS, Mullighan CG, Ma J, Wheeler DA, Hampton OA, Ross N, Gastier-Foster JM, Arold ST, Perlman EJ. A children's Oncology group and target initiative exploring the genetic landscape of Wilms tumor. *Nat Genet* 2017;49:1487–94.
13 Wu MK, Sabbaghian N, Xu B, Addidou-Kalucki S, Bernard C, Zou D, Reeve AE, Eccles MR, Cole C, Choong CS, Charles A, Tan TY, Iglesias DM, Goodyer PR, Foulkes WD. Biallelic DICER1 mutations occur in Wilms tumours. *J Pathol* 2013;230:154–64.
14 Zehir A, Benayed R, Shah RH, Syed A, Middha S, Kim HR, Srinivasan P, Gao J, Chakravarty D, Devlin SM, Hellmann MD, Barron DA, Schram AM, Hameed M, Dogan S, Ross DS, Hechtman JF, DeLair DF, Yao J, Mandelker DL, Cheng DT, Chandramohan R, Mohanty AS, Ptashkin RN, Jayakumaran G, Prasad M, Syed MH, Rema AB, Liu ZY, Nafa K, Borsu L, Sadowska J, Casanova J, Bacares R, Kiecka IJ, Razumova A, Son JB, Stewart L, Baldi T, Mullaney KA, Al-Ahmadie H, Vakiani E, Abeshouse AA, Penson AV, Jonsson P, Camacho N, Chang MT, Won HH, Gross BE, Kundra R, Heins ZJ, Chen H-W, Phillips S, Zhang H, Wang J, Ochoa A, Wills J, Eubank M, Thomas SB, Gardos SM, Reales DN, Galle J, Durany R, Cambria R, Abida W, Cercek A, Feldman DR, Gounder MM, Hakimi AA, Harding JJ, Iyer G, Janjigian YY, Jordan EJ, Kelly CM, Lowery MA, Morris LGT, Omuro AM, Raj N, Razavi P, Shoushtari AN, Shukla N, Soumerai TE, Varghese AM, Yaeger R, Coleman J, Bochner B, Riely GJ, Saltz LB, Scher HI, Sabbatini PJ, Robson ME, Klimstra DS, Taylor BS, Baselga J, Schultz N, Hyman DM, Arcila ME, Solit DB, Ladanyi M, Berger MF. Mutational landscape of metastatic cancer revealed from prospective clinical sequencing of 10,000 patients. *Nat Med* 2017;23:703–13.
15 Tate JG, Bamford S, Jubb HC, Sondka Z, Beare DM, Bindal N, Boutselakis H, Cole CG, Creatore C, Dawson E, Fish P, Harsha B, Hathaway C, Jupe SC, Kok CY, Noble K, Ponting L, Ramshaw CC, Rye CE, Speedy HE, Stefancsik R, Thompson SL, Wang S, Ward S, Campbell PJ, Forbes SA. Cosmic: the Catalogue of somatic mutations in cancer. *Nucleic Acids Res* 2019;47:D941–7.
16 de Kock L, Bah I, Wu Y, Xie M, Priest JR, Foulkes WD. Germline and somatic DICER1 mutations in a well-differentiated fetal adenocarcinoma of the lung. *J Thorac Oncol* 2016;11:e31–3.
17 Wu Y, Chen D, Li Y, Bian L, Ma T, Xie M. DICER1 mutations in a patient with an ovarian Sertoli-Leydig tumor, well-differentiated fetal adenocarcinoma of the lung, and familial multinodular goiter. *Eur J Med Genet* 2014;57:621–5.
18 Liu S, Wang J, Luo X, Li X, Miao Y, Wang L, Li Q, Qiu X, Wang E-H. Coexistence of low-grade fetal adenocarcinoma and adenocarcinoma in situ of the lung harboring different genetic mutations: a case report and review of literature. *Onco Targets Ther* 2020;13:6675–80.
19 Khan NE, Bauer AJ, Doros L, Schultz KAP, Decastro RM, Harney LA, Kase RG, Carr AG, Harris AK, Williams GM, Dehner LP, Messinger YH, Stewart DR. Macrocephaly associated with the DICER1 syndrome. *Genet Med* 2017;19:244–8.
20 Klein SD, Martinez-Agosto JA. Hotspot mutations in DICER1 causing GLOW Syndrome-associated macrocephaly *via* modulation of specific microRNA populations results in activation of PI3K/ATK/mTOR signaling. *Microrna* 2020;9:70–80.
21 de Kock L, Hillmer M, Wagener R, Soglio DB-D, Sabbaghian N, Siebert R, Priest JR, Miller M, Foulkes WD. Further evidence that full gene deletions of DICER1 predispose to DICER1 syndrome. *Genes Chromosomes Cancer* 2019;58:602–4.
22 Herriges JC, Brown S, Longhurst M, Ozmore J, Moeschler JB, Janze A, Meck J, South ST, Andersen EF. Identification of two 14q32 deletions involving DICER1 associated with the development of DICER1-related tumors. *Eur J Med Genet* 2019;62:9–14.
23 de Kock L, Geoffrion D, Rivera B, Wagener R, Sabbaghian N, Bens S, Ellezam B, Bouron-Dal Soglio D, Ordóñez J, Sacharow S, Polo Nieto JF, Guillerman RP, Vujanic GM, Priest JR, Siebert R, Foulkes WD. Multiple DICER1-related tumors in a child with a large interstitial 14q32 deletion. *Genes Chromosomes Cancer* 2018;57:223–30.
24 van Engelen K, Villani A, Wasserman JD, Aronoff L, Greer M-LC, Tijerin Bueno M, Gallinger B, Kim RH, Grant R, Meyn MS, Malkin D, Druker H. Dicer1 syndrome: approach to testing and management at a large pediatric tertiary care center. *Pediatr Blood Cancer* 2018;65.
25 Zampini L, D'Odorico L, Zanchi P, Zollino M, Neri G. Linguistic and psychomotor development in children with chromosome 14 deletions. *Clin Linguist Phon* 2012;26:962–74.
26 Ting TW, Brett MS, Cham BWM, Lim J-Y, Law HY, Tan EC, Lai AHM, Jamuar SS. DICER1 deletion and 14q32 microdeletion syndrome: an additional case and a review of the literature. *Clin Dysmorphol* 2016;25:37–40.
27 Piccione M, Antona V, Scavone V, Malacarne M, Pierluigi M, Grasso M, Corsello G. Array CGH defined interstitial deletion on chromosome 14: a new case. *Eur J Pediatr* 2010;169:845–51.

Supplementary Table 1; *List of analyzed genes*

HGNC symbol	HGNC ID	Description
ABCA12	14637	ATP binding cassette subfamily A member 12
ABCC9	60	ATP binding cassette subfamily C member 9
ACAN	319	aggrecan
ACOX1	119	acyl-CoA oxidase 1
ADK	257	adenosine kinase
AGGF1	24684	angiogenic factor with G-patch and FHA domains 1
AHI1	21575	Abelson helper integration site 1
AKT1	391	AKT serine/threonine kinase 1
AKT3	393	AKT serine/threonine kinase 3
ALX3	449	ALX homeobox 3
ALX4	450	ALX homeobox 4
AMER1	26837	APC membrane recruitment protein 1
ANKH	15492	ANKH inorganic pyrophosphate transport regulator
ANTXR2	21732	ANTXR cell adhesion molecule 2
AP1S2	560	adaptor related protein complex 1 subunit sigma 2
APC2	24036	APC2 WNT signaling pathway regulator
ARL13B	25419	ADP ribosylation factor like GTPase 13B
ARL6	13210	ADP ribosylation factor like GTPase 6
ARMC9	20730	armadillo repeat containing 9
ARSB	714	arylsulfatase B
ARVCF	728	ARVCF delta catenin family member
ASPA	756	aspartoacylase
ASXL2	23805	ASXL transcriptional regulator 2
B3GALNT2	28596	beta-1 3-N-acetylgalactosaminyltransferase 2
B3GALT6	17978	beta-1 3-galactosyltransferase 6
B3GLCT	20207	beta 3-glucosyltransferase
B4GALT1	924	beta-1 4-galactosyltransferase 1
B4GALT7	930	beta-1 4-galactosyltransferase 7
B4GAT1	15685	beta-1 4-glucuronyltransferase 1
B9D1	24123	B9 domain containing 1
B9D2	28636	B9 domain containing 2
BBIP1	28093	BBSome interacting protein 1
BBS1	966	Bardet-Biedl syndrome 1
BBS10	26291	Bardet-Biedl syndrome 10
BBS12	26648	Bardet-Biedl syndrome 12
BBS2	967	Bardet-Biedl syndrome 2
BBS4	969	Bardet-Biedl syndrome 4
BBS5	970	Bardet-Biedl syndrome 5
BBS7	18758	Bardet-Biedl syndrome 7
BBS9	30000	Bardet-Biedl syndrome 9
BGN	1044	biglycan
BHLHA9	35126	basic helix-loop-helix family member a9
BLM	1058	BLM RecQ like helicase
BMP2	1069	bone morphogenetic protein 2
BMP4	1071	bone morphogenetic protein 4
BMPR1B	1077	bone morphogenetic protein receptor type 1B
BRAF	1097	B-Raf proto-oncogene serine/threonine kinase
BRCA2	1101	BRCA2 DNA repair associated

BRWD3	17342	bromodomain and WD repeat domain containing 3
BUB1	1148	BUB1 mitotic checkpoint serine/threonine kinase
BUB1B	1149	BUB1 mitotic checkpoint serine/threonine kinase B
BUB3	1151	BUB3 mitotic checkpoint protein
C12orf57	29521	chromosome 12 open reading frame 57
C2CD3	24564	C2 calcium dependent domain containing 3
C8orf37	27232	chromosome 8 open reading frame 37
CAMTA1	18806	calmodulin binding transcription activator 1
CC2D2A	29253	coiled-coil and C2 domain containing 2A
CCDC22	28909	coiled-coil domain containing 22
CCND2	1583	cyclin D2
CD96	16892	CD96 molecule
CDC45	1739	cell division cycle 45
CDC73	16783	cell division cycle 73
CDCA7	14628	cell division cycle associated 7
CDKN1C	1786	cyclin dependent kinase inhibitor 1C
CEP104	24866	centrosomal protein 104
CEP120	26690	centrosomal protein 120
CEP164	29182	centrosomal protein 164
CEP290	29021	centrosomal protein 290
CEP41	12370	centrosomal protein 41
CEP55	1161	centrosomal protein 55
CEP57	30794	centrosomal protein 57
CFC1	18292	cripto FRL-1 cryptic family 1
CHD4	1919	chromodomain helicase DNA binding protein 4
CHD7	20626	chromodomain helicase DNA binding protein 7
CHN1	1943	chimerin 1
CHRNA7	1960	cholinergic receptor nicotinic alpha 7 subunit
CLCN7	2025	chloride voltage-gated channel 7
COG6	18621	component of oligomeric golgi complex 6
COL25A1	18603	collagen type XXV alpha 1 chain
COL2A1	2200	collagen type II alpha 1 chain
COL4A1	2202	collagen type IV alpha 1 chain
COLEC10	2220	collectin subfamily member 10
COMT	2228	catechol-O-methyltransferase
CPLX1	2309	complexin 1
CRB2	18688	crumbs cell polarity complex component 2
CREBBP	2348	CREB binding protein
CSPP1	26193	centrosome and spindle pole associated protein 1
CTBP1	2494	C-terminal binding protein 1
CUL4B	2555	cullin 4B
CWC27	10664	CWC27 spliceosome associated protein homolog
D2HGDH	28358	D-2-hydroxyglutarate dehydrogenase
DACT1	17748	dishevelled binding antagonist of beta catenin 1
DAG1	2666	dystroglycan 1
DDX59	25360	DEAD-box helicase 59
DEAF1	14677	DEAF1 transcription factor
DHCR24	2859	24-dehydrocholesterol reductase
DHCR7	2860	7-dehydrocholesterol reductase
DICER1	17098	dicer 1 ribonuclease III
DIS3L2	28648	DIS3 like 3'-5' exoribonuclease 2

DLL3	2909	delta like canonical Notch ligand 3
DMRT3	13909	doublesex and mab-3 related transcription factor 3
DNMT3A	2978	DNA methyltransferase 3 alpha
DNMT3B	2979	DNA methyltransferase 3 beta
DOCK6	19189	dedicator of cytokinesis 6
DPYD	3012	dihydropyrimidine dehydrogenase
DVL1	3084	dishevelled segment polarity protein 1
DVL3	3087	dishevelled segment polarity protein 3
DYNC2H1	2962	dynein cytoplasmic 2 heavy chain 1
DYNC2LI1	24595	dynein cytoplasmic 2 light intermediate chain 1
EBP	3133	EBP cholestenol delta-isomerase
EED	3188	embryonic ectoderm development
EFNB1	3226	ephrin B1
EFTUD2	30858	elongation factor Tu GTP binding domain containing 2
EIF2B1	3257	eukaryotic translation initiation factor 2B subunit alpha
EIF2B2	3258	eukaryotic translation initiation factor 2B subunit beta
EIF2B3	3259	eukaryotic translation initiation factor 2B subunit gamma
EIF2B4	3260	eukaryotic translation initiation factor 2B subunit delta
EIF2B5	3261	eukaryotic translation initiation factor 2B subunit epsilon
EML1	3330	EMAP like 1
EP300	3373	E1A binding protein p300
ERF	3444	ETS2 repressor factor
ERMARD	21056	ER membrane associated RNA degradation
ETFA	3481	electron transfer flavoprotein subunit alpha
ETFB	3482	electron transfer flavoprotein subunit beta
ETFDH	3483	electron transfer flavoprotein dehydrogenase
EVC	3497	EvC ciliary complex subunit 1
EVC2	19747	EvC ciliary complex subunit 2
EXT2	3513	exostosin glycosyltransferase 2
EZH2	3527	enhancer of zeste 2 polycomb repressive complex 2 subunit
FAM111A	24725	family with sequence similarity 111 member A
FANCB	3583	FA complementation group B
FBLN1	3600	fibulin 1
FBN1	3603	fibrillin 1
FGF10	3666	fibroblast growth factor 10
FGFR1	3688	fibroblast growth factor receptor 1
FGFR2	3689	fibroblast growth factor receptor 2
FGFR3	3690	fibroblast growth factor receptor 3
FGFRL1	3693	fibroblast growth factor receptor like 1
FH	3700	fumarate hydratase
FIBP	3705	FGF1 intracellular binding protein
FKRP	17997	fukutin related protein
FKTN	3622	fukutin
FLI1	3749	Fli-1 proto-oncogene ETS transcription factor
FLII	3750	FLII actin remodeling protein
FLNA	3754	filamin A
FMR1	3775	fragile X mental retardation 1
FOXP1	3823	forkhead box P1
FOXRED1	26927	FAD dependent oxidoreductase domain containing 1
FZD2	4040	frizzled class receptor 2
GABRD	4084	gamma-aminobutyric acid type A receptor delta subunit

GATA4	4173	GATA binding protein 4
GATA6	4174	GATA binding protein 6
GCDH	4189	glutaryl-CoA dehydrogenase
GDF1	4214	growth differentiation factor 1
GDF5	4220	growth differentiation factor 5
GDF6	4221	growth differentiation factor 6
GFAP	4235	glial fibrillary acidic protein
GJA1	4274	gap junction protein alpha 1
GJB6	4288	gap junction protein beta 6
GLI1	4317	GLI family zinc finger 1
GLI2	4318	GLI family zinc finger 2
GLI3	4319	GLI family zinc finger 3
GNAI3	4387	G protein subunit alpha i3
GNAQ	4390	G protein subunit alpha q
GNAS	4392	GNAS complex locus
GP1BB	4440	glycoprotein Ib platelet subunit beta
GPC3	4451	glypican 3
GPC4	4452	glypican 4
GRIA3	4573	glutamate ionotropic receptor AMPA type subunit 3
GUSB	4696	glucuronidase beta
H19	4713	H19 imprinted maternally expressed transcript
HDAC4	14063	histone deacetylase 4
HDAC6	14064	histone deacetylase 6
HELLS	4861	helicase lymphoid specific
HEPACAM	26361	hepatic and glial cell adhesion molecule
HERC1	4867	HECT and RLD domain containing E3 ubiquitin protein ligase family member 1
HES7	15977	hes family bHLH transcription factor 7
HESX1	4877	HESX homeobox 1
HEXB	4879	hexosaminidase subunit beta
HIRA	4916	histone cell cycle regulator
HIST1H1E	4718	histone cluster 1 H1 family member e
HNRNPK	5044	heterogeneous nuclear ribonucleoprotein K
HOXA13	5102	homeobox A13
HOXD13	5136	homeobox D13
HRAS	5173	HRas proto-oncogene GTPase
HSD17B4	5213	hydroxysteroid 17-beta dehydrogenase 4
HUWE1	30892	HECT UBA and WWE domain containing 1 E3 ubiquitin protein ligase
HYLS1	26558	HYLS1 centriolar and ciliogenesis associated
ICK	21219	intestinal cell kinase
IDS	5389	iduronate 2-sulfatase
IDUA	5391	iduronidase alpha-L-
IFT140	29077	intraflagellar transport 140
IFT172	30391	intraflagellar transport 172
IFT27	18626	intraflagellar transport 27
IFT43	29669	intraflagellar transport 43
IFT52	15901	intraflagellar transport 52
IFT74	21424	intraflagellar transport 74
IFT80	29262	intraflagellar transport 80
IFT81	14313	intraflagellar transport 81
IGBP1	5461	immunoglobulin binding protein 1
IGF2	5466	insulin like growth factor 2

IHH	5956	Indian hedgehog signaling molecule
INPP5E	21474	inositol polyphosphate-5-phosphatase E
INPPL1	6080	inositol polyphosphate phosphatase like 1
INTU	29239	inturned planar cell polarity protein
IQSEC2	29059	IQ motif and Sec7 domain 2
ISPD	37276	isoprenoid synthase domain containing
ITCH	13890	itchy E3 ubiquitin protein ligase
JMJD1C	12313	jumonji domain containing 1C
KCNAB2	6229	potassium voltage-gated channel subfamily A regulatory beta subunit 2
KCNJ1	6255	potassium voltage-gated channel subfamily J member 1
KCNJ8	6269	potassium voltage-gated channel subfamily J member 8
KCNQ1	6294	potassium voltage-gated channel subfamily Q member 1
KCNQ1OT1	6295	KCNQ1 opposite strand/antisense transcript 1
KDM1A	29079	lysine demethylase 1A
KDM5C	11114	lysine demethylase 5C
KIAA0556	29068	KIAA0556
KIAA0586	19960	KIAA0586
KIAA0753	29110	KIAA0753
KIF22	6391	kinesin family member 22
KIF7	30497	kinesin family member 7
KLLN	37212	killin p53 regulated DNA replication inhibitor
KPTN	6404	kaptin actin binding protein
KRAS	6407	KRAS proto-oncogene GTPase
L1CAM	6470	L1 cell adhesion molecule
L2HGDH	20499	L-2-hydroxyglutarate dehydrogenase
LAMB1	6486	laminin subunit beta 1
LARGE1	6511	LARGE xylosyl- and glucuronyltransferase 1
LBR	6518	lamin B receptor
LETM1	6556	leucine zipper and EF-hand containing transmembrane protein 1
LFNG	6560	LFNG O-fucosylpeptide 3-beta-N-acetylglucosaminyltransferase
LHX4	21734	LIM homeobox 4
LMBR1	13243	limb development membrane protein 1
LRP2	6694	LDL receptor related protein 2
LRP4	6696	LDL receptor related protein 4
LRP5	6697	LDL receptor related protein 5
LZTFL1	6741	leucine zipper transcription factor like 1
MAB21L2	6758	mab-21 like 2
MAFB	6408	MAF bZIP transcription factor B
MAN2B1	6826	mannosidase alpha class 2B member 1
MAP2K1	6840	mitogen-activated protein kinase kinase 1
MAP2K2	6842	mitogen-activated protein kinase kinase 2
MAP3K1	6848	mitogen-activated protein kinase kinase kinase 1
MAPK10	6872	mitogen-activated protein kinase 10
MBTPS2	15455	membrane bound transcription factor peptidase site 2
MECP2	6990	methyl-CpG binding protein 2
MED12	11957	mediator complex subunit 12
MEGF8	3233	multiple EGF like domains 8
MESP2	29659	mesoderm posterior bHLH transcription factor 2
MGAT2	7045	mannosyl (alpha-1 6-)-glycoprotein beta-1 2-N-acetylglucosaminyltransferase
MITF	7105	melanocyte inducing transcription factor
MKKS	7108	McKusick-Kaufman syndrome

MKS1	7121	Meckel syndrome type 1
MLC1	17082	megalencephalic leukoencephalopathy with subcortical cysts 1
MOCS1	7190	molybdenum cofactor synthesis 1
MOCS2	7193	molybdenum cofactor synthesis 2
MPDZ	7208	multiple PDZ domain crumbs cell polarity complex component
MSX2	7392	msh homeobox 2
MTM1	7448	myotubularin 1
MTOR	3942	mechanistic target of rapamycin kinase
MYH8	7578	myosin heavy chain 8
NDUFA1	7683	NADH:ubiquinone oxidoreductase subunit A1
NDUFA11	20371	NADH:ubiquinone oxidoreductase subunit A11
NDUFAF1	18828	NADH:ubiquinone oxidoreductase complex assembly factor 1
NDUFAF2	28086	NADH:ubiquinone oxidoreductase complex assembly factor 2
NDUFAF3	29918	NADH:ubiquinone oxidoreductase complex assembly factor 3
NDUFAF4	21034	NADH:ubiquinone oxidoreductase complex assembly factor 4
NDUFAF5	15899	NADH:ubiquinone oxidoreductase complex assembly factor 5
NDUFB3	7698	NADH:ubiquinone oxidoreductase subunit B3
NDUFB9	7704	NADH:ubiquinone oxidoreductase subunit B9
NDUFS1	7707	NADH:ubiquinone oxidoreductase core subunit S1
NDUFS2	7708	NADH:ubiquinone oxidoreductase core subunit S2
NDUFS3	7710	NADH:ubiquinone oxidoreductase core subunit S3
NDUFS4	7711	NADH:ubiquinone oxidoreductase subunit S4
NDUFS6	7713	NADH:ubiquinone oxidoreductase subunit S6
NDUFV1	7716	NADH:ubiquinone oxidoreductase core subunit V1
NDUFV2	7717	NADH:ubiquinone oxidoreductase core subunit V2
NEK1	7744	NIMA related kinase 1
NEK9	18591	NIMA related kinase 9
NELFA	12768	negative elongation factor complex member A
NF1	7765	neurofibromin 1
NFIA	7784	nuclear factor I A
NFIX	7788	nuclear factor I X
NKX2-5	2488	NK2 homeobox 5
NKX2-6	32940	NK2 homeobox 6
NKX3-2	951	NK3 homeobox 2
NLRC4	16412	NLR family CARD domain containing 4
NLRP3	16400	NLR family pyrin domain containing 3
NOTCH2	7882	notch 2
NPHP1	7905	nephrocystin 1
NPHP3	7907	nephrocystin 3
NR0B1	7960	nuclear receptor subfamily 0 group B member 1
NR5A1	7983	nuclear receptor subfamily 5 group A member 1
NRAS	7989	NRAS proto-oncogene GTPase
NSD1	14234	nuclear receptor binding SET domain protein 1
NSD2	12766	nuclear receptor binding SET domain protein 2
NUBPL	20278	nucleotide binding protein like
NXN	18008	nucleoredoxin
OFD1	2567	OFD1 centriole and centriolar satellite protein
OPHN1	8148	oligophrenin 1
OTX2	8522	orthodenticle homeobox 2
PALB2	26144	partner and localizer of BRCA2
PAX6	8620	paired box 6

PDE6D	8788	phosphodiesterase 6D
PDSS1	17759	decaprenyl diphosphate synthase subunit 1
PEX1	8850	peroxisomal biogenesis factor 1
PEX10	8851	peroxisomal biogenesis factor 10
PEX11B	8853	peroxisomal biogenesis factor 11 beta
PEX12	8854	peroxisomal biogenesis factor 12
PEX13	8855	peroxisomal biogenesis factor 13
PEX14	8856	peroxisomal biogenesis factor 14
PEX16	8857	peroxisomal biogenesis factor 16
PEX19	9713	peroxisomal biogenesis factor 19
PEX2	9717	peroxisomal biogenesis factor 2
PEX26	22965	peroxisomal biogenesis factor 26
PEX3	8858	peroxisomal biogenesis factor 3
PEX5	9719	peroxisomal biogenesis factor 5
PEX6	8859	peroxisomal biogenesis factor 6
PHF21A	24156	PHD finger protein 21A
PHF6	18145	PHD finger protein 6
PHF8	20672	PHD finger protein 8
PIBF1	23352	progesterone immunomodulatory binding factor 1
PIGA	8957	phosphatidylinositol glycan anchor biosynthesis class A
PIGN	8967	phosphatidylinositol glycan anchor biosynthesis class N
PIGT	14938	phosphatidylinositol glycan anchor biosynthesis class T
PIK3CA	8975	phosphatidylinositol-4 5-bisphosphate 3-kinase catalytic subunit alpha
PIK3R2	8980	phosphoinositide-3-kinase regulatory subunit 2
PITX1	9004	paired like homeodomain 1
PLCB4	9059	phospholipase C beta 4
PLG	9071	plasminogen
PNPLA6	16268	patatin like phospholipase domain containing 6
POC1A	24488	POC1 centriolar protein A
POLE	9177	DNA polymerase epsilon catalytic subunit
POMGNT1	19139	protein O-linked mannose N-acetylglucosaminyltransferase 1 (beta 1 2-)
POMGNT2	25902	protein O-linked mannose N-acetylglucosaminyltransferase 2 (beta 1 4-)
POMK	26267	protein-O-mannose kinase
POMT1	9202	protein O-mannosyltransferase 1
POMT2	19743	protein O-mannosyltransferase 2
POP1	30129	POP1 homolog ribonuclease P/MRP subunit
PORCN	17652	porcupine O-acyltransferase
POU1F1	9210	POU class 1 homeobox 1
POU6F2	21694	POU class 6 homeobox 2
PPP2R5D	9312	protein phosphatase 2 regulatory subunit B'delta
PRDM16	14000	PR/SET domain 16
PROP1	9455	PROP paired-like homeobox 1
PTCH1	9585	patched 1
PTCH2	9586	patched 2
PTDSS1	9587	phosphatidylserine synthase 1
PTEN	9588	phosphatase and tensin homolog
PTHLH	9607	parathyroid hormone like hormone
RAB23	14263	RAB23 member RAS oncogene family
RAB39B	16499	RAB39B member RAS oncogene family
RAC1	9801	Rac family small GTPase 1
RAI1	9834	retinoic acid induced 1

RBM10	9896	RNA binding motif protein 10
RERE	9965	arginine-glutamic acid dipeptide repeats
REST	9966	RE1 silencing transcription factor
RIPPLY2	21390	ripply transcriptional repressor 2
RIT1	10023	Ras like without CAAX 1
RNF125	21150	ring finger protein 125
RNF135	21158	ring finger protein 135
ROR2	10257	receptor tyrosine kinase like orphan receptor 2
RPGRIP1	13436	RPGR interacting protein 1
RPGRIP1L	29168	RPGRIP1 like
RREB1	10449	ras responsive element binding protein 1
RUNX2	10472	runt related transcription factor 2
SALL1	10524	spalt like transcription factor 1
SALL4	15924	spalt like transcription factor 4
SC5D	10547	sterol-C5-desaturase
SDCCAG8	10671	serologically defined colon cancer antigen 8
SDHB	10681	succinate dehydrogenase complex iron sulfur subunit B
SDHC	10682	succinate dehydrogenase complex subunit C
SDHD	10683	succinate dehydrogenase complex subunit D
SEC23A	10701	Sec23 homolog A coat complex II component
SEC23B	10702	Sec23 homolog B coat complex II component
SEC24C	10705	SEC24 homolog C COPII coat complex component
SEC24D	10706	SEC24 homolog D COPII coat complex component
SEMA3E	10727	semaphorin 3E
SERPINH1	1546	serpin family H member 1
SETBP1	15573	SET binding protein 1
SETD2	18420	SET domain containing 2
SH2B1	30417	SH2B adaptor protein 1
SHANK3	14294	SH3 and multiple ankyrin repeat domains 3
SHH	10848	sonic hedgehog signaling molecule
SHOC2	15454	SHOC2 leucine rich repeat scaffold protein
SHPK	1492	sedoheptulokinase
SIM1	10882	SIM bHLH transcription factor 1
SKI	10896	SKI proto-oncogene
SLC25A1	10979	solute carrier family 25 member 1
SLC26A2	10994	solute carrier family 26 member 2
SLC29A3	23096	solute carrier family 29 member 3
SLC2A10	13444	solute carrier family 2 member 10
SLC35D1	20800	solute carrier family 35 member D1
SMARCB1	11103	SWI/SNF related matrix associated actin dependent regulator of chromatin subfamily b member 1
SMO	11119	smoothened frizzled class receptor
SMOC1	20318	SPARC related modular calcium binding 1
SNX10	14974	sorting nexin 10
SNX14	14977	sorting nexin 14
SOS1	11187	SOS Ras/Rac guanine nucleotide exchange factor 1
SOST	13771	sclerostin
SOX9	11204	SRY-box 9
SPINT2	11247	serine peptidase inhibitor Kunitz type 2
SPRED1	20249	sprouty related EVH1 domain containing 1
SRY	11311	sex determining region Y
STRADA	30172	STE20 related adaptor alpha

SUFU	16466	SUFU negative regulator of hedgehog signaling
SUMF1	20376	sulfatase modifying factor 1
SUZ12	17101	SUZ12 polycomb repressive complex 2 subunit
SYN1	11494	synapsin I
TBCK	28261	TBC1 domain containing kinase
TBX1	11592	T-box 1
TBX15	11594	T-box 15
TBX3	11602	T-box 3
TBX6	11605	T-box 6
TCF12	11623	transcription factor 12
TCIRG1	11647	T cell immune regulator 1 ATPase H+ transporting V0 subunit a3
TCTEX1D2	28482	Tctex1 domain containing 2
TCTN1	26113	tectonic family member 1
TCTN2	25774	tectonic family member 2
TCTN3	24519	tectonic family member 3
TFAP2A	11742	transcription factor AP-2 alpha
TFAP2B	11743	transcription factor AP-2 beta
TGFBR1	11772	transforming growth factor beta receptor 1
TGFBR2	11773	transforming growth factor beta receptor 2
THRA	11796	thyroid hormone receptor alpha
TIMMDC1	1321	translocase of inner mitochondrial membrane domain containing 1
TMCO1	18188	transmembrane and coiled-coil domains 1
TMEM107	28128	transmembrane protein 107
TMEM126B	30883	transmembrane protein 126B
TMEM138	26944	transmembrane protein 138
TMEM216	25018	transmembrane protein 216
TMEM231	37234	transmembrane protein 231
TMEM237	14432	transmembrane protein 237
TMEM67	28396	transmembrane protein 67
TNFRSF11A	11908	TNF receptor superfamily member 11a
TNFRSF11B	11909	TNF receptor superfamily member 11b
TNFSF11	11926	TNF superfamily member 11
TP53	11998	tumor protein p53
TRAF3IP1	17861	TRAF3 interacting protein 1
TRIM32	16380	tripartite motif containing 32
TRIM37	7523	tripartite motif containing 37
TRIP11	12305	thyroid hormone receptor interactor 11
TRIP13	12307	thyroid hormone receptor interactor 13
TTC21B	25660	tetratricopeptide repeat domain 21B
TTC8	20087	tetratricopeptide repeat domain 8
TWIST1	12428	twist family bHLH transcription factor 1
UBE2A	12472	ubiquitin conjugating enzyme E2 A
UBE3A	12496	ubiquitin protein ligase E3A
UFD1	12520	ubiquitin recognition factor in ER associated degradation 1
UPF3B	20439	UPF3B regulator of nonsense mediated mRNA decay
UQCC2	21237	ubiquinol-cytochrome c reductase complex assembly factor 2
USP9X	12632	ubiquitin specific peptidase 9 X-linked
VAMP7	11486	vesicle associated membrane protein 7
WASHC5	28984	WASH complex subunit 5
WDPCP	28027	WD repeat containing planar cell polarity effector
WDR19	18340	WD repeat domain 19

WDR34	28296	WD repeat domain 34
WDR35	29250	WD repeat domain 35
WDR60	21862	WD repeat domain 60
WNT5A	12784	Wnt family member 5A
WNT7A	12786	Wnt family member 7A
WT1	12796	Wilms tumor 1
WWOX	12799	WW domain containing oxidoreductase
XYLT1	15516	xylosyltransferase 1
YME1L1	12843	YME1 like 1 ATPase
ZBTB20	13503	zinc finger and BTB domain containing 20
ZBTB24	21143	zinc finger and BTB domain containing 24
ZBTB42	32550	zinc finger and BTB domain containing 42
ZDHHC9	18475	zinc finger DHHC-type containing 9
ZFPM2	16700	zinc finger protein FOG family member 2
ZIC1	12872	Zic family member 1
ZIC3	12874	Zic family member 3
ZNF141	12926	zinc finger protein 141
ZNF423	16762	zinc finger protein 423
ZNF469	23216	zinc finger protein 469
ZSWIM6	29316	zinc finger SWIM-type containing 6

Supplementary Table 2; *Sequence variants correlating to patient phenotype*

HGNC symbol, sequence variant
DICER1, NM_030621 (ENST00000393063) c.4031C>T p.Ser1344Leu, heterozygous
GLI2, NM_005270 (ENST00000361492) c.1760C>T p.Thr587Met, heterozygous
LRP5, NM_002335 (ENST00000294304) c.3552C>T p.=, heterozygous
LRP5, NM_002335 (ENST00000294304) c.4466C>T p.Thr1489Met, heterozygous

Supplementary Table 3.
WT bearing RNase IIIa/IIIb hotspot mutations

	PUBLICATION			WT PATIENT INFORMATION		GERMLINE/MOSAIC DICER1 VARIANT				WILMS TUMOR/SOMATIC DICER1 MUTATION				NUMBER OF DICER1 MUTATIONS
	Reference	*PMID*	*Year*	*Case ID, age, sex*	*Phenotype*	*Exon*	*DNA change*	*Protein change*	*Domain*	*Exon*	*DNA change*	*Protein change*	*Domain*	
1	Pontén *et al.*	this case	2020	Swedish patient; 15 months, male	WT, WFDLA, Type I PPB, CN, ID, Macrocephaly	21	c.4031C>T	p.S1344L	RNase IIIa		0.61 Mb deletion spanning *DICER1*			Two mutations
2	Carlens *et al.*	conference pamphlet	2018	German patient; 11 months, female	WT, ID, LC bilateral, Macrocephaly	21	c.4031C>T	p.S1344L	RNase IIIa		Not analyzed			Tumor status unknown
3	Foulkes *et al.*	24676357	2011	Fam4:III-2; 4 years, male	WT	8	c.912_919dup	p.R307Qfs*8	TRBPBD	21	c.4031C>T	p.S1344L	RNase IIIa	Two mutations
4	Gadd *et al.*	28825729	2017	PAJNPI; 2,6 years, male	WT					21 + 17	c.4031C>T + c.2771T>G	p.S1344L + p.L924*	RNase IIIa	Two mutations
5	Klein *et al.*	24676357	2014	Case 1; 9 months, male	WT, LC bilateral, DD, OGS (GLOW syndrome)	24	c.5138A>T (mosaic)	p.D1713V (mosaic)	RNase IIIb	8 + 27	c.1304C>A + c.5692A>G	p.P453H + p.R1898G	Helicase C-Terminal + dsRBD	Two mutations
6	Klein *et al.*	24676357	2014	Case 2; 18 months, male	WT, LC bilateral, DD, OGS (GLOW syndrome)	24	c.5125G>T (mosaic)	p.D1709Y (mosaic)	RNase IIIb		No other mutation			Monoallelic
7	Foulkes *et al.*	24676357	2011	Fam5:II-1; 2 years, male	WT	8	c.1306dup	p.S436Ffs*41	btwn TRBPBD and HELICc	25	c.5138A>C	p.D1713A	RNase IIIb	Two mutations
8	Foulkes *et al.*	24676357	2011	Fam3:IV-3; 5 years	WT, MNG	intron 13/junction exon 14	c.2117-1G>A	p.G706Afs*8	DUF	24	c.5429A>G	p.D1810G	RNase IIIb	Two mutations
9	Rakheja *et al.*	25190313	2014	CMCW11; 5,2 years, female	WT, ASK, Thyroid-FA, ERMS, SLCT bilateral	21	c.3307_3311del	p.I1102fsdel	btwn PAZ and RNase IIIa	25	c.5425G>A	p.G1809R	RNase IIIb	Two mutations
10	Wu *et al.*	23620094	2013	Case N	WT					25	c.5438A>G + c.5452G>A	p.E1813G + p.A1818T	exon 25 skip + RNase IIIb	Two mutations
11	Gadd *et al.*	28825729	2017	PAJNRH; 3,7 years + 4 years, female	WT bilateral?					27 + 24	c.5622C>G + c.5125G>A	p.Y1874* + p.D1709N	dsRBD + RNase IIIb	Two mutations
12	Gadd *et al.*	28825729	2017	PAJLVL; 5,4 years, female	WT					24 + 6	c.5138A>T + c.734+1T>C	p.D1713V + NMD	RNase IIIb	Two mutations
13	Gadd *et al.*	28825729	2017	PAKJJF; 3,2 years, female	WT					19 + 24	c.3008G>A + c.5125G>A	p.R1003Q + p.D1709N	PAZ + RNase IIIb	Two mutations
14	Walz *et al.*	25670082	2015	ValidationSetFHWT5	WT					24	c.5125G>	p.D1709N	RNase IIIb	Monoallelic
15	Walz *et al.*	25670082	2015	ValidationSetFHWT6	WT					24	c.5125G>	p.D1709N	RNase IIIb	Monoallelic
16	Gadd *et al.*	28825729	2017	PAJLXH; 8,3 years, female	WT					24	c.5125G>A	p.D1709N	RNase IIIb	Monoallelic
17	Gadd *et al.*	28825729	2017	PAJMWN; 2,1 years, female	WT					25	c.5125G>A	p.D1709N	RNase IIIb	Monoallelic
18	Walz *et al.*	25670082	2015	ValidationSetFHWT3	WT					24	c.5113G>	p.E1705K	RNase IIIb	Monoallelic
19	Walz *et al.*	25670082	2015	ValidationSetFHWT4	WT					24	c.5113G>	p.E1705K	RNase IIIb	Monoallelic

20	Gadd *et al.*	28825729	2017	PAJNBW; 2,6 years, female	WT		24	c.5113G>A	p.E1705K	RNase IIIb	Monoallelic
21	Gadd *et al.*	28825729	2017	PAJPAH; 3 years, female	WT		24	c.5113G>A	p.E1705K	RNase IIIb	Monoallelic
22	Gadd *et al.*	28825729	2017	PALEZT; 12 years, female	WT		24	c.5113G>A	p.E1705K	RNase IIIb	Monoallelic
23	Gadd *et al.*	28825729	2017	PAJLML; 3,9 years, male	WT		25	c.5428G>A	p.D1810N	RNase IIIb	Monoallelic
24	Gadd *et al.*	28825729	2017	PAJMVL; 2,7 years, male	WT		25	c.5428G>A	p.D1810N	RNase IIIb	Monoallelic
25	Torrezan *et al.*	24909261	2014	ACC13	WT		25	c.5428G>A	p.D1810N	RNase IIIb	Monoallelic
26	Walz *et al.*	25670082	2015	ValidationSetFHWT8	WT		25	c.5428G>	p.D1810N	RNase IIIb	Monoallelic
27	Walz *et al.*	25670082	2015	ValidationSetFHWT9	WT		25	c.5428G>	p.D1810N	RNase IIIb	Monoallelic
28	Walz *et al.*	25670082	2015	ValidationSetFHWT7	WT		25	c.5138A>	p.D1713V	RNase IIIb	Monoallelic
29	Rakheja *et al.*	25190313	2014	CMCW59; 3,5 years, male	WT		25	c.5426G>T	p.G1809V	RNase IIIb	Monoallelic

Abbreviations: ASK, anaplastic sarcoma of the kidney; CN, cystic nephroma; DD, developmental delay; ERMS, embryonal rhabdomyosarcoma; ID, intellectual disability; MNG, multinodular goitre; PPB, pleuropulmonary blastoma; OGS, overgrowth syndrome; LC, lung cysts; SLCT, Sertoli-Leydig cell tumor; Thyroid-FA, thyroid follicular adenoma; WT, Wilms tumor; WDFLA, well differentiated fetal lung carcinoma dsRBD, double stranded RNA binding domain; DUF, domain of unknown function, TRBPBD, TAR RNA binding protein binding domain.

Number of Cases	Description
4	p.S1344L
29	WT bearing a *DICER1* RNase IIIa/IIIb hotspot mutation*
11	WT bearing two *DICER1* alterations
17	WT bearing a single *DICER1* RNase IIIa/IIIb hotspot alteration
1	WT bearing germline *DICER1* RNase IIIa mutation; tumor status not known

**p.E1705, p.D1709, p.G1809, p.D1810, p.E1813, p.D1713, p.S1344L*